Mapping of resistance loci in wheat line Milan/S87230//Babax to South African races of *Puccinia striiformis* f. sp. *tritici*

Renée Prins (cengen@cengen.co.za)
CenGen Pty Ltd and Stellenbosch University https://orcid.org/0000-0001-9775-6709
Corneli de Klerk
CenGen Pty Ltd
Willem H.P. Boshoff
University of the Free State
Cornel M Bender
University of the Free State
Zacharias A Pretorius
University of the Free State
Kirsty S Botha
CenGen Pty Ltd
Elsabet Wessels
CenGen Pty Ltd

Research Article

Keywords: Stripe rust resistance, QTL mapping, wheat, Yr17

Posted Date: July 21st, 2022

DOI: https://doi.org/10.21203/rs.3.rs-1877247/v1

Abstract

The continuous emergence of new *Puccinia striiformis* Westend f. sp. *tritici* Erikss (*Pst*) races requires a sustained search for useful sources of resistance. A CIMMYT bread wheat line (pedigree: Milan/S87230//Babax; renamed NSRPan4) was identified as highly resistant to South African *Pst* races. A recombinant inbred line (RIL) mapping population was developed by crossing NSRPan4 with Avocet S. Stripe rust data collected for RILs, using *Pst* race 6E22A+, include seedling infection types determined under controlled conditions as well as adult plant responses determined in field trials over three consecutive seasons. Quantitative trait loci (QTL) mapping identified stripe rust resistance genes/QTL on chromosomes 2A and 2B, temporarily designated as *QYr.ufs-2A.2(Yr17)* and *QYr.ufs-2B.1*, respectively. The QTL interval on chromosome 2A, which includes the *Lr37/Yr17/Sr38* gene complex (also referred to as the 2NS/2AS or $2N^{V}S$ segment), conferred a significant seedling (R^2 23.5%) and adult plant resistance effect (R^2 up to 54.5%). The QTL on 2B contributed up to 46.4% of phenotypic variance observed. Three minor QTL, temporarily designated as *QYr.ufs-1B.1* (possibly *Lr46/Yr29*), *QYr.ufs-3D.1* and *QYr.ufs-7A.1* were also detected. Our results support findings that notwithstanding the reported virulence for *Yr17*, the *Lr37/Yr17/Sr38* segment remains useful in combination with other sources of resistance in certain genetic backgrounds and environments. Together with *QYr.ufs-2B.1* and in the presence of the detected minor QTL and yet unidentified resistances, it was a consistent major contributor to the high level of stripe rust resistance in NSRPan4 to South African races of *Pst*.

Introduction

Stripe (yellow) rust, caused by *Puccinia striiformis* Westend f. sp. *tritici* Erikss (*Pst*), presents a global threat to wheat (*Triticum aestivum* L.) yields, especially in cool and moist production regions. The more recent occurrence of the disease in traditionally warmer and drier areas has compounded the impact of stripe rust, (Walter et al. 2016). Wheat producers in South Africa (SA) rely on a combination of control strategies to combat the disease. These include planting of resistant cultivars, fungicide seed treatment and foliar sprays. The occurrence of epidemic outbreaks and high disease incidence in commercial wheat fields after the first observation of stripe rust in SA in 1996 emphasised the economic importance of the disease (Pretorius et al. 2007). To mitigate the risk of future epidemic outbreaks the continuous identification and incorporation of new sources of resistance, effective against prevailing races of *Pst*, are important.

Sources of stripe rust resistance are broadly classified as all-stage (ASR) and adult plant (APR) (Line and Chen 1995; McIntosh et al. 1995; Chen 2013). APR is considered more durable and expressed at later growth stages (Qayoum and Line 1985; Chen 2013, 2020), and is generally more sought-after than ASR detected from the early seedling stage throughout the plant's life span and which tends to be overcome more easily due to its race-specific nature. In general, seedling stage resistance is often attributed to a single locus with little environmental influence, whilst APR is often considered to be due to multiple loci and affected by the environment. Fang et al. (2011), however issued a note of caution in generalising when it comes to this perception. The availability of genome sequence information and associated knowledge allow for examples which challenge these strict criteria. An example was the cloning of *Yr27* (previously *QYr.sgi-2B.1*) that showed moderate seedling resistance and strong APR to the South African *Pst* race 6E22A + and which contributes to the near-immune phenotype observed in the field for wheat cultivar Kariega (Athiyannan et al. 2022).

Research to dissect the genetics of APR towards wheat stripe rust has resulted in the identification of many quantitative trait loci (QTL) and associated DNA markers (Ramburan et al. 2004; Prins et al. 2011; Agenbag et al. 2012, 2014; Rosewarne et al. 2013). The designated and temporarily designated genes for *Pst* are catalogued at shigen (https://shigen.nig.ac.jp/wheat/komugi/genes/symbolClassList.jsp; Li et al. 2020). Furthermore, many loci have received temporary designations in addition to all the major and minor effect resistance QTL that have been identified all over the world (McIntosh et al. 2017; Wang and Chen, 2017).

At CIMMYT (International Maize and Wheat Improvement Centre), the development of rust resistant wheat cultivars, with an emphasis on combining genes expressing resistance in adult plants, is a major objective (Bhavani et al. 2019; Huerta-Espino et al. 2020; Juliana et al. 2020). The success of the CIMMYT Global Wheat Program in releasing high-yielding wheat varieties with durable rust resistance, abiotic stress tolerance and acceptable quality traits (Guzmán et al. 2017), is underlined by the fact that these varieties are currently sown on 60 million hectares worldwide (https://www.cimmyt.org/work/wheat-research/ accessed 26 February 2021).

In addition to productive varieties, CIMMYT compiles nurseries which are globally distributed and screened for desirable traits, including under South African conditions. Entry 110 of the 28th Elite Spring Wheat Yield Trial (ESWYT) (pedigree: Milan/S87230//Babax) was identified for further study based on its consistently high level of resistance (near-immune phenotype) displayed under local field conditions of excessive stripe rust pressure. In a comprehensive study of the genetics of stripe rust resistance in CIMMYT lines, Juliana et al. (2020) concluded that Milan, occurring in the pedigree of the above-mentioned line, was the parent genotype contributing *Yr17* to lines carrying the *Yr.cim-2AS.1* QTL. *Yr17* was introduced from *Aegilops ventricosa* via the gene-rich $2N^{v}S$ translocation to wheat (McIntosh et al. 1995; Gao et al. 2021). Based on seedling tests on control lines such as Trident and *Yr17*/6*AvS, *Yr17* is considered ineffective against South African races of *Pst* (Visser et al. 2016), therefore the 0R field phenotype necessitates further investigation. In further support of this study, it was stated that although *Yr17* was classified as an ASR resistance gene, *Pst* isolates exist that are considered avirulent on adult plants and then unexpectedly producing intermediate to high seedling infection types (SITs) on the same plants (Milus et al. 2015). Apart from temperature, wheat genotype, *Pst* isolate and leaf stage that influenced SIT the authors argued that intermediate SITs likely represent a level of partial virulence in the pathogen that is insufficient to cause disease on adult plants in the field. Similarly, Fang et al. (2011) concluded in their study of seedling and adult plant stripe rust resistance phenotypes conferred by the 2NS/2AS segment in Jagger that *Yr17* has an APR effect in response to some pathotypes supporting the notion that this gene can be considered a race-specific APR gene. The objective of this study was thus to analyse the genetics of resistance to stripe rust in 28th ESWYT line 110 as a potential source of stripe rust resistance in SA by first following a cost-effective low genomic coverage approach to identify putative QTL regions before incurring the investment required for a fine mapping effort.

Materials And Methods

Plant material

Line 110 from the 28th ESWYT (renamed NSRPan4) was crossed with Avocet S (stripe rust-susceptible) to develop a recombinant inbred line (RIL) population (n = 167) through single-seed descent. In 2014 seed of F_6 lines were split for multiplication and the first rust assessment in the field. In 2015 and 2016 F_7 RILs were used for seedling and field evaluations. Concurrent with RIL development, F_2 and BC_1F_2 families were advanced. Trident (*Lr37*/*Yr17*/*Sr38*) and *Yr5*/6*Avocet S were used as additional DNA marker controls.

Field evaluation of disease resistance

Field plots were planted at the Redgates Research Facility of PANNAR SEED (Pty) Ltd., Greytown, SA in 2012, 2014, 2015 and 2016. F_2 and BC_1F_2 families of NSRPan4 x Avocet S were evaluated in 2012. F_2 seeds were space-planted to allow for single plant assessments. The stripe rust-susceptible wheat lines JIC871 and Morocco were alternated at 20-row intervals to serve as susceptible checks. In addition, a mixture of susceptible cultivars was planted as stripe rust spreader rows at intervals along the length of the trial site. Prior to planting, 250 kg 2:3:4 (38) N-P-K plus 0.5% Zn fertilizer was broadcasted per hectare. Supplemental sprinkler irrigation was applied when necessary. In all years a stripe rust epidemic was created by inoculating susceptible checks with *Pst* pathotype 6E22A+ early in the season. One hundred and sixty-seven F_6 or F_7 lines of the NSRPan4 x Avocet S population, and duplicate entries of the parents, were planted in 2014, 2015 and 2016. One replication was planted in 2014 and 2016 whereas two replicates were evaluated in 2015. For the 2015 season, the average score of the two replicates were used in the QTL analysis. All field plots were 1 m in length, spaced 75 cm apart.

F_2 plants were individually scored as resistant (R) or susceptible (S) whereas BC_1F_2 families were rated on a row basis as either segregating or susceptible. Disease severity (DS) was visually scored according to the modified Cobb Scale (Peterson et al. 1948; (0-100%)) and reported as leaf area infected (LAI) and host reaction type (RT) as R, RMR (resistant to moderately resistant), MR (moderately resistant), MRMS (moderately resistant to moderately susceptible), MS (moderately susceptible) MSS (moderately susceptible to susceptible) and S. For statistical purposes these categories, and interpolations, were converted to a 1-7 ordinal scale (Ramburan et al. 2004; Agenbag et al. 2012). Stripe rust assessment of RILs was done at two occasions in all years. In 2014 and 2016 RIL plots were also assessed for leaf damage using a handheld GreenSeeker® (GS) crop sensor (model HCS 100) according to the methods described by Pretorius et al. (2017). The sensor gives a normalised difference vegetation index (NDVI) for each row. For QTL analysis these scores were converted to (1-NDVI)*100. In 2014 NDVI ratings were taken nine days before the final visual phenotyping whereas in 2016 both traits were assessed on the same day.

As part of routine field work conducted by University of the Free State (UFS) researchers, stripe rust phenotypes of control lines and international nurseries are recorded at the Greytown trial site annually. For this study the field response (FR) of lines containing *Yr17* in particular was noted.

Seedling tests

Five to 10 plants of each NSRPan4 x Avocet S F_7 RIL as well as of the parents were tested for their SIT to pathotype 6E22A+ of *Pst*. Entries were sown in clumps of five seeds in commercial Mikskaar® potting medium in 10 cm diameter pots. After sowing pots were kept in a growth cabinet at 23°C for 3 days to ensure equal emergence of seedlings before placement in a greenhouse cubicle at 18-25°C. Primary leaves of 7-day-old plants were inoculated with urediniospores suspended in Soltrol-130 light mineral oil. Plants were allowed to dry for 1 h before they were incubated at high humidity for 24 h. The dew chamber (two were used) consisted of a galvanized metal sheeting box which was placed inside a cold room at 10°C. Hot water (~40°C) was added to the bottom of each chamber, to a level below an expanded metal grid supporting pots, just before enclosing the plants. The lids of the chambers were sealed with tape. On completion of the dew period, seedlings were kept at 17°C in a growth chamber for 18 h before they were transferred to a greenhouse cubicle maintained at 15-20°C. SITs were recorded 14 days post-inoculation according to a “0” - “4” scale (McIntosh et al. 1995). Control lines NSRPan4, Avocet S and Trident were also inoculated with *Pst* pathotypes 6E16A-, 6E22A- and 6E22A+.

SITs were determined over three independent replicates. Considering all data sets, the most commonly occurring phenotype was documented for each entry. These consensus SITs were transformed according to a 1-9 scale (SIT_1-9) as previously proposed (Prins et al. 2011) and used in the QTL analysis (Online Resource 1). The relationship between SIT (X-axis) and FR traits was visualised using box plots (Online Resource 2) (NCSS ver. 8 Statistical Analysis and Graphics software). The boxes displayed for each SIT class signify the inter-quartile data range for each field trait. Means of LAI, RT and GS over the respective seasons were used. The horizontal line within each box represents the median. Whisker boundaries were determined by multiplying the inter-quartile range by a factor of 1.5 and outliers are designated by dots.

Molecular marker analysis, linkage map construction, QTL analysis and comparison with physical map positions

Genomic DNA was extracted from the 167 RIL F_6 lines using an adapted cetyltrimethyl ammonium bromide (CTAB) DNA extraction protocol (Doyle and Doyle 1990). Extracted DNA was quantified with a NanoDrop® Spectrophotometer ND-1000 and all samples were diluted to a 25 ng/ul working concentration.

Similar to most QTL mapping studies done in the pre-Next Generation Sequencing era (Wessels et al. 2019; Jaganathan et al. 2020), a cost-effective low genomic coverage approach was followed to first identify putative QTL regions. Parental lines were subjected to a Low-Resolution Genome Scan (LRGS) consisting of a selection of 104 microsatellite (SSR) markers, spread across the hexaploid wheat genome, covering all 21 chromosomes (Wessels and Prins 2017) to identify potential chromosome areas of importance for stripe rust resistance QTL. Following the first rounds of linkage and QTL mapping, the crossing parents were also typed with 243 additional markers. This included SSR markers mostly for 1B, 2A, and 2B, KASP™ single-nucleotide polymorphism (SNPs) markers and markers associated with *Yr5* (2B) and *Lr37/Yr17/Sr38* (2A), targeting the significant chromosome areas identified in the preliminary analysis. All SSR typing was performed using fluorescent primers in multiplex polymerase chain reactions (PCR) and PCR products were analysed on a 3730*xl* Genetic Analyzer (Applied Biosystems) at the Central Analytical Facility at Stellenbosch University (http://www.sun.ac.za/english/faculty/science/CAF/units/dna-sequencer). GeneScan™ 500 LIZ® was used as an internal size standard and the marker data were analysed using GeneMapper v4.0 (Applied Biosystems) software. KASP™ primer sequences were obtained from CerealsDB (https://www.cerealsdb.uk.net/cerealgenomics/CerealsDB/kasp_mapped_snps.php; Wilkinson et al. 2012) and all SNP reactions were performed in 384-well format with dried template DNA as per manufacturer's protocol. The total reaction volume per sample was 3.041 ul and a standard 63-57°C touchdown PCR program was followed as indicated in the KASP™ genotyping chemistry user guide and manual (available at http://www.lgcgroup.com/products/kasp-genotyping-chemistry/). The data were analysed in KlusterKaller v1.05 (KBiosciences). An SSR marker, gwm501, reported to be 10.5-13.3 cM from *Yr5* (Sun et al. 2002) was included in the marker screen. In addition, the presence of *Yr5* was also screened for with an amplified fragment length polymorphism (AFLP) derived sequence-tagged site (STS) marker, S19M93-100 (Smith et al. 2007), on a real-time PCR platform (CFX96 Touch; Bio-Rad). In a 10 µl reaction, the PCR components were 50 ng of template DNA, 5 pmol of S19M93-100 forward and reverse primer, a final concentration of 1 x KAPA HRM FAST Master Mix (Kapa Biosystems), 2.5 mM $MgCl_2$ and ddH_2O to bring up the volume. The positive control for the *Yr5* gene was an *Yr5*/6*Avocet S line (obtained from the Agricultural Research Council - Small Grains). The following PCR conditions were used: 3 min at 95°C followed by 40 cycles of 5 seconds (sec) at 95°C and 30 sec at 64°C. A melt step was performed: 1 min at 95°C, 10 sec at 40°C, 70-90°C with a temperature increase of 0.2°C/sec and finally 10 min at 40°C. Unlabelled primers Ventriup and LN2 were used to screen for *Lr37/Yr17/Sr38* (Helguera et al. 2003) and is referred to as the *Lr37/Yr17/Sr38* marker in this study. In a 10 ul reaction, the PCR components were 50 ng of template DNA, 3 pmol of forward and reverse primer, a final concentration of 1 x KAPA2G Fast ReadyMix with dye (Kapa Biosystems) and ddH_2O to make up the volume. Trident was used as the positive control for *Lr37/Yr17/Sr38*. The following PCR conditions were used: 3 min at 95°C, 34 cycles of 95°C for 15 sec, 68°C for 15 sec, 72°C for 1 sec and a final extension step of 10 min at 72°C. The PCR products were visualized on a 1.5% agarose gel with an ethidium bromide concentration of 0.05% using a UVIpro Platinum high performance gel documentation system (Whitehead Scientific).

A total of 202 informative markers (yielding 237 informative loci; Online Resource 1) were typed in the RIL population and linkage groups were constructed as in Agenbag et al. (2012). Composite interval mapping (CIM) was performed with Windows QTL Cartographer v2.51 (Wang et al. 2012), using a forward and backward regression model, a window size of 10 cM and a walk speed of 1 cM. A 1000 permutations were performed (p = 0.05) for all the phenotypic data sets to determine the logarithm of the odds (LOD) threshold above which a QTL was considered as significant. MapChart V2.3 (Voorrips 2002) was used to illustrate the maps.

The SSR- and KASP™ marker order for the most significant QTL regions obtained in our mapping study was compared to the order of these markers according to their physical map positions. By focussing on recombination events in NSRPan4, the size and position of the regions of interest for stripe rust resistance were delimited. Basic Local Alignment Search Tool (BLAST) searches on the Ensembl Plants website (https://plants.ensembl.org/Multi/Tools/Blast) with the forward primers as query sequences were used to determine the markers' physical positions on the Chinese Spring RefSeq v1.0 assembly (IWGSC 2018) and the Jagger – a known $2N^VS$ translocation carrier – PGSB v2.0 genome assembly (Walkowiak et al. 2020) (the latter only for the QTL on 2A). Physical positions were only assigned to markers with 100% exact matches on the chromosomes of interest and markers were arranged according to these positions on the genome(s). Many of the SSR and KASP™ markers in the regions of interest on chromosomes 2A and 2B produced null alleles in either NSRPan4 or Avocet S (Online Resource 3), thereby indicating the loss of a primer binding site and possible recombination. This, along with the BLAST results, was used to determine the most likely physical order of markers on the target chromosomes of NSRPan4 and to infer the physical size of the regions of interest.

Analysis of parental lines and a selection of RILs on a 35K Affymetrix Axiom™ Wheat Breeders' Array

The parental lines and a selection of RILs were also included on a 35K Affymetrix Axiom™ Wheat Breeders' Array (Allen et al. 2017) to gain further insight into the major QTL regions identified (Table 1). Two different seed sources (2014 and 2019) of RILs#157 and #163 which unexpectedly exhibited a number of cross-overs in the 2A QTL interval were included. Initial quality analysis of the data was performed in the Axiom™ Analysis Suite v5.1.1.1 (www.thermofisher.com) using the Best Practises Workflow and the Axiom_WhtBrd-1.r4 array package. The following parameters for SNP calling were applied: Average call rate for passing samples ≥ 97%; QC call rate ≥95%, and dish quality control (DQC) ≥ 81%. An inbred penalty of 10 was applied to the parental lines (inbred lines) and of 5 to all RIL lines to account for heterozygosity at the F_6/F_7 generations. The ProbeSets were further filtered for those with high quality cluster plots ("PolyHighResolution", "OTV", and "NoMinorHom") and with a Minor Allele Frequency > 0.05. After the application of these quality parameters, the data for all remaining ProbeSets were exported for further analysis.

Downstream data processing was executed in R v4.0.5 using RStudio v1.4.1106 (R Core Team 2013). Axiom^{TM} ProbeSets that were monomorphic between the parental lines or had a heterozygous or "NoCall" allele call in these two lines were filtered out. The genotypic calls of the RILs were coded according to their similarity to the parental lines' calls: "A" if equal to the NSRPan4 call and "B" if equal to Avocet S. Heterozygous or "NoCall" data were coded with a dash ("-"). In a final filtering step, Axiom^{TM} ProbeSets located within the QTL regions on the physical map were selected. The R-package ggplot2 (Wickham 2016) was used to plot the coded data according to the physical map positions on the chromosomes from the short arm (top) to the long arm (bottom). SSR and KASP^{TM} marker order was included on the plot in two ways: a) according to the physical positions of the markers as discussed above, b) in the order of the QTL mapping results. To plot the markers from the mapping results on the same physical scale, the physical distances between the markers were calculated proportionally to the genetic map distances between them, using the corresponding flanking markers as anchoring points.

Results

Phenotypes

In all field experiments the final DS of NSRPan4 was rated as trace R as opposed to 100S for Avocet S. Field data of 223 F_2 plants ($\chi^2_{15:1}$ = 1.187, p = 0.276) and BC_1F_2 ($\chi^2_{3:1}$ = 0.055, p = 0.815), rated in 2012 during construction of the RILs, showed a highly significant fit for a two-gene model. F_2 phenotypes of plants considered to express some form of resistance varied from trace R to 70MSS, with intermediate severities in the MR, MRMS and MS response categories. Ten plants scored 80MS or higher and were considered susceptible. A similar range of stripe rust responses was recorded amongst the BC_1F_2 families with 42 segregating and 13 being susceptible. RILs varied from highly R, similar to the NSRPan4 phenotype, through the intermediate or partially resistant categories, to full susceptibility.

The stripe rust phenotype of wheat line *Yr17*/6*Avocet S included in the 6th to 10th Yellow Rust Trap Nursery (YRTN), was rated as 70MRMS (2012), 30MS (2014), 80MRMS (2015) and 50MRMS (2016) (unpublished data; ZA Pretorius). The corresponding Avocet S entry from the same nursery was rated as 100S in all years. In 2016, two sources of the wheat cultivar Trident (Australian and UFS stem rust differential series) both scored 30R on the same day as the final assessment of the mapping population.

In the seedling assay NSRPan4 consistently displayed a ;1c SIT. Avocet S was fully susceptible (SIT 4). SITs of individual RILs covered the entire phenotype scale and varied from ;c to 4. When the parents were compared with Trident, all isolates produced the typical ;1c response on NSRPan4 while Avocet S and the *Yr17* control were susceptible (Fig. 1).

The field responses of RILs ranged from R, RMR, MRMS, MSS to S with severities of trace to 100 (Online Resources 1 and 4). The LAI and RT box plots, in general, showed an increase in field susceptibility with higher SITs (Online Resource 2a, b). However, some RILs showed low LAI and/or a low RT despite transformed seedling response categories of 7 and higher (3 to 4 on the regular scale). The opposite was also true as some RILs with low to intermediate seedling responses were associated with higher than expected leaf damage. The GS plot was not as informative but showed that NDVI values indicative of susceptibility, were associated with SIT categories 7 - 9 (Online Resource 2).

Linkage maps

Ninety-six of the LRGS markers (~92%), 95 of the additional SSR markers (~46%) and 16 of the KASP^{TM} SNPs (~46%) were informative in the parental lines. Combined, the SSRs (some multi-locus), KASP^{TM} SNPs and gene-specific markers, yielded a total of 237 informative marker loci which produced 30 linkage groups (p = 1.0e-6) representing 20 wheat chromosomes (Fig. 2, 3; Online Resource 5) according to the wheat consensus map (Appels 2003). Chromosome 4A is not represented in the linkage map used in the analysis. Twenty loci representing a variety of linkage groups remained unlinked. In this population, the STS-marker S19M93-100 for *Yr5* (2B) amplified a similar peak (melting temp of 84.0-85.0°C) to the *Yr5*/6*Avocet S control line but in the RILs it mapped to the linkage group representing chromosome 2D, whilst gwm501 mapped to its expected position on 2B (Fig. 3). Amplification of the *Yr17* gene was obtained with the Ventriup and LN2 primers which confirmed the presence of this translocation segment in NSRPan4 and was mapped as *Lr37/Yr17/Sr38* to the distal part of the short arm in linkage group 2A (Helguera et al. 2003; Fig. 2).

QTL analysis

Following the permutation test, LOD significance thresholds at 95% for all 15 traits ranged from 2.6-3.0. Considering the SIT, FR (LAI; RT) and GS responses, CIM revealed five NRSPan4 chromosomes of interest: 2A, 2B and 1B, 3D and 7A (Table 2). Single marker regression with the unlinked markers (spread over chromosomes 1D, 2A, 3A, 3B, 3D, 4A, 5A, 5B, 5D, 6D, 7A, 7B, 7D) did not detect any association with any phenotypic scores.

The most consistent effect was seen in a fairly large 24 cM region on chromosome 2AS (temporarily designated *QYr.ufs-2A.2(Yr17))* which was significant for all of the phenotypic scores (Fig. 2). As expected, when comparing the map with Helguera et al. (2003), the *Lr37/Yr17/Sr38* associated marker mapped to the

most terminal part of this chromosomal region. The R^2 for severity (LAI) ranged from 19.4-54.5%; 31.0-48.6% for RT; 19.3-40.3% for GS and was 23.5% for SIT_1-9 (Table 2). The most significantly linked marker locus across the evaluated traits varied in the gwm210a to gwm210b region within the larger gwm210a-gwm512 interval.

Another region of significance (temporarily designated *QYr.ufs-2B.1*) was detected on chromosome 2BL in the interval between gwm501 and wmc317 (Fig. 3). It was significant among all the scores except in the early season LAI score of 2016 (Table 2). The R^2 for LAI ranged from 6.5-16.3%; 11.1-27.1% for RT, 6.1-13.9% for GS and was 46.4% for SIT_1-9. This significant area spans a region of approximately 45 cM with the QTL peak consistently the highest at marker BS00022064 (except for GS_07OCT14 with BS000110209 as the most significantly associated marker).

A smaller effect was observed on chromosome 1B (*QYr.ufs-1B.1)*, only significant for the end of season LAI and RT scores in 2015 and 2016 and the GS score of 2016 (Table 2). The maximum variance explained was 13.2% for RT_01OCT15. The most significant markers were cfa2219a and wmc44 within the larger interval of cfa2219a-barc80, placing it in the region where the multipathogen *Lr46/Yr29* resistance gene maps on the distal part of 1BL (Suenaga et al. 2003; Rosewarne et al. 2006) as represented by linkage group 1B.2 in this study (Online Resource 5).

Minor effects were detected for *QYr.ufs-3D.1* (3D) and *QYr.ufs-7A.1* (7A). *QYr.ufs-3D.1* (3D) was only significant for one RT score (R^2 = 5.3%) and for the SIT score (SIT_1-9) (R^2 = 6.4%) while *QYr.ufs-7A.1* was only detected in one LAI score (R^2 = 5.0%). Markers cfd4 (3D) and wmc422 (7A) were the closest linked markers to the significant QTL peaks. These QTL designations will be used until their relationship with known genes can be determined. In 2014 NDVI ratings were taken nine days before the final visual phenotyping (thus on 7OCT14) whereas in 2016 both LAI and NDVI traits were assessed on the same day (thus on 29SEP16). Both NDVI ratings detected *QYr.ufs-2A.2(Yr17)* and *QYr.ufs-2B.1,* but *QYr.ufs-1B.1* was only observed with GS_29SEPT16 which was taken on the same day as the LAI_29SSEPT16 rating. In the comparisons of the mean phenotypes of specific subsets, the NDVI rating followed the same trend as the LAI readings (Online Resource 2). These findings support a previous study that Greenseeker® readings are an accurate indication of the disease severity (LAI) (Pretorius et al. 2017) and can be used to speed up phenotyping.

The *QYr.ufs-2A.2(Yr17)* markers anchored to the Chinese Spring and Jagger genomes

Several SSR markers in the *QYr.ufs-2A.2(Yr17)* QTL region produced null alleles in either Avocet S or NSRPan4 (Online Resource 3). By comparing the physical positions of these markers on chromosome 2A of Chinese Spring and Jagger respectively, the relative size and position of the QTL region on NSRPan4 were inferred (Online Resource 3). Markers with partial or no BLAST matches to chromosome 2A of Chinese Spring or Jagger (gdm5 and gpw2018) were excluded from the map comparisons. Additionally, the marker delimiting the QTL interval in the mapping study, gwm210, had no match to Jagger 2A and an exact match to only one position on Chinese Spring 2A, despite mapping to more than one position on this chromosome in this study and was therefore excluded from the map comparisons as well. Xib125c, the most terminal marker on both Chinese Spring 2A and Jagger 2A, did not amplify an allele in NSRPan4 and it was therefore not clear whether NSRPan4 carries an allele for this multi-locus marker similar to Chinese Spring or Jagger. Apart from this marker and as expected, NSRPan4 displayed a marker profile like Jagger (a known 2NS/2AS carrier; Fang et al 2011) in the terminal region of chromosome 2AS containing the *Lr37/Yr17/Sr38* associated marker, BS00021691, gpw4108 and BS00053661 – a 29,021,202 bp region in Jagger. The marker on the distal end of the QTL region, gwm512, had a 100% match to Chinese Spring at 12,168,808 bp and produced a null allele in NSRPan4, indicating that the primer binding site was most likely replaced by the wild relative chromatin in NSRPan4. Marker wmc25c, also with 100% match to Chinese Spring, produced a null allele in Avocet S and a 191 bp fragment in NSRPan4, most likely signifying the putative breakpoint between *T. aestivum* and *A. ventricosa* chromatin in NSRPan4. From gwm359 towards the centromere the NSRPan4 and Jagger marker profiles were similar to that of Chinese Spring and Avocet S (Online Resource 3). Avocet S displayed a marker profile like Chinese Spring (markers which produced PCR fragments and with 100% matches to this genome), except for two markers, xib58 and wmc25c, that produced null alleles in Avocet S but had matches to 2A of Chinese Spring.

The *QYr.ufs-2B.1* markers anchored to the Chinese Spring genome

Gwm501 flanking the *QYr.ufs-2B.1* region, is also a marker associated with *Yr5*, and produced a null allele in NSRPan4. For KASP™ markers BS00009989 and BS00110209 the forward primer that amplified the NSRPan4 allele had a mismatch with the Chinese Spring genome on the last base pair of the primers. BS00110209 is the most distal flanking marker of the *QYr.ufs-2B.1* interval. The forward primer of SSR marker cfd267b did not produce any BLAST hit on the Chinese Spring genome. The reverse primer produced a full match on chromosome 2A and an 80% match on chromosome 2B at position 681,331,064. Save from this marker, all other markers in the *QYr.ufs-2B.1* region were in the same order on the physical map than on the genetic map produced in this study. The region of interest between flanking markers BS00110209 and wmc317 is 38.8 Mb in size.

35K Affymetrix Axiom™ Wheat Breeders' Array analysis

All samples submitted for Axiom™ analysis passed QC analysis and 13,640 SNP markers were subsequently exported for downstream analysis. The data confirmed that the two seed sources (2014 and 2019) for RIL#157 and RIL#163 were identical, however producing many NoCalls (failed PCR) and

heterozygous (AB) calls on all of the group 2 chromosomes of RIL#157 and chromosome 2A of RIL#163.

Eighty-six Axiom^{TM} ProbeSets were located within the 20,544,761 bp region of interest (using xib125c, the most terminal marker on 2A, and wmc25c, the probable break point of the translocation, as delimiting markers for ProbeSet selection) on chromosome 2A with IWGSC RefSeq v1.0 of Chinese Spring as reference genome (IWGSC 2018). Of these, 71 were polymorphic between the two parental lines. Compared to the high number of null alleles detected with the SSR markers (Online Resource 3), only five ProbeSets within the region of interest on 2A were classified as "OTV" (SNP null alleles) by the Axiom^{TM} Analysis Suite.. All lines previously called, based on the SSR data, as carrying the *QYr.ufs-2A.2 (Yr17)* QTL had the same allele calls as NSRPan4 for Axiom^{TM} ProbeSets in the physical region of the QTL (Online Resource 6).

Two-hundred and fifty-two ProbeSets were located within the larger *QYr.ufs-2B.1* QTL region between markers gwm501 (672,082,697) and wmc317 (784,343,192). 121 of these ProbeSets were polymorphic between the two parental lines, of which 34 are located between flanking markers BS00110209 (745,579,661) and wmc317. All lines previously called, based on the SSR data, as containing *QYr.ufs-2B.1* had the same allele call as NSRPan4 for Axiom^{TM} ProbeSets in the physical region of KASP^{TM} marker BS00022064, the marker most significantly associated with the resistance for most traits (Online Resource 7). Although a number of NoCalls and heterozygous calls were produced in the *QYr.ufs-2B.1* area of RIL#165, it was not disproportionately more than the other lines when taking the entire genome into consideration and therefore the integrity of the lines is not doubted.

Discussion

The near-immune stripe rust response of wheat line NSRPan4 (Milan/S87230//Babax), first detected in a CIMMYT nursery in 2007, was expressed across three seasons of field testing in SA. This highly resistant phenotype was consistently displayed against *Pst* pathotype 6E22A + under conditions of extreme disease pressure. A line with the same pedigree as NSRPan4 showed 5MRMS to stripe rust in Pakistan (Shah 2015) and low RTs and severities at two screening nurseries in Washington State, USA in 2013 (https://striperust.wsu.edu/nursery-data/2013-nursery-data/) (accessed 20 February 2022). In Northern India where this line has been released as cultivar WH1105, a slow rusting phenotype was observed (https://bgri.cornell.edu/; https://www.globalrust.org/taxonomy/term/626/all). In the current study, the *Lr37/Yr17/Sr38* segment from NSRPan4, provided partial seedling and APR to *Pst* pathotype 6E22A+. Evidence of the latter includes RILs with the *Lr37/Yr17/Sr38* segment that displayed < 30% LAI and R to RMR RTs over seasons despite intermediate (2+) to high (4) SITs. The total phenotypic variance (R^2) for LAI and RT explained by the detected QTL varied according to the timing of ratings within a season and across seasons, underlining the effect of environmental influences on the expression of the detected QTL (Table 2). This may partly explain the conflicting reports on the resistance observed in Milan/S87230//Babax in different countries and underpins the environmental and genetic background effects for the *Lr37/Yr17/Sr38* segment as reviewed by Milus et al. (2015). In addition to these effects, it is highly probable that this line will respond differently to other *Pst* pathotypes as have been found in several studies with material containing the 2N^{V}S segment. In addition to the reports of virulence for *Yr17* in Europe and other regions (Bayles et al. 2000; Sharma-Poudyal et al. 2013), Juliana et al. (2020) found in a comprehensive genome wide association study that it was only effective against races in Mexico and earlier Kenya-Njoro trials, but ineffective at Njoro since 2015–2016 and India.

In the 2016 season the total R^2 varied from 19.4–64.8% between the early and late LAI score. In general, the total R^2 observed in the 2015 season (up to 71.6%) was the highest compared to 2014 and 2016, reflecting the higher R^2 explained by *QYr.ufs-2A.2* (including *Lr37/Yr17/Sr38*) for both field scores (LAI and RT). Fang et al. (2011) showed that *QYr.osu-2A* (representing the *Yr17* segment in Jagger) surprisingly explained 80 to 93% of the phenotypic variation in adult plants in different environments in the USA, allowing natural infection with pathotypes reportedly virulent on *Yr17*. Only 36% of the variance could be explained when tested in the field in China with pathotype CYR32. The latter is also reported to be virulent on *Yr17* (Fang et al. 2011) The SIT_1–9 score together with the early season RT score in 2016 detected a QTL (*QYr.ufs.3D-1*) in addition to the two major areas on 2A and 2B, which brought the total R^2 value for SIT_1–9 up to 76.3%. This was the highest total R^2 value observed. Little or no seedling resistance was found to segregate in the RIL: Jagger (*Lr37/Yr17/Sr38*-carrier*)* x 2174 mapping population studied by Fang et al. (2011).

Although the representation of four to five markers per linkage group is probably not sufficient to detect linkage with minor QTL, we were successful in discovering two main and one minor chromosome regions conferring stripe rust resistance to NSRPan4. The QTL analysis' detection (2014–2016) of two main chromosome regions of interest (2A and 2B) was supported by field data of F_2 and BC_1F_2 segregating material obtained in 2012 during construction of the RILs which showed a significant fit for a two-gene model. With up to 71.6% of total phenotypic variance explained for LAI and 76.3% for SIT_1–9 it is also possible that some minor resistance remains undetected due to the very sparse map where most linkage groups were represented by only four markers.

Based on pedigree analysis, it can be concluded that the *Lr37/Yr17/Sr38* translocated segment in NSRPan4 was introduced via the VPM1-derivative, Milan, which carries the translocated 2N^{V}S *Aegilops ventricosa Tausch* (syn. *T. ventricosum Tausch* (Ces)) segment (Bariana and McIntosh 1993, Maia 1967 as cited in Cruz et al. 2016; Gao et al. 2021). The *Lr37/Yr17/Sr38* associated marker was amongst the markers in the 24.3 cM *QYr.ufs-2A.2(Yr17)* interval most significantly linked with the variance observed in seedling and adult plant responses (Table 2, Fig. 2). Helguera et al. (2003) mapped the *Lr37/Yr17/Sr38* gene complex in the 2AS translocated region with the two outermost RFLP loci being *Xcmwg682* (distal) and *XksuH9* (proximal). The distance between these two loci was inferred from the 2A^{m}S map of *T. monococcum* (Dubcovsky et al. 1996) to be approximately 25–38 cM, while it covers a distance of ~ 16 cM in the wheat consensus map (Appels 2003). From the marker haplotype data for this interval (Online Resource 3) it seems that the 29 Mb translocated segment in NSRPan4 is represented by the *Lr37/Yr17/Sr38* marker up to wmc25c, which falls within the most distal section of chromosome 2AS, is situated 13 cM from the telomeric end on the wheat consensus map (Appels 2003), and well within the *Xcmg682 - XksuH9a* interval as reported by Helguera et al. (2003). In a Jagger x 2174 RIL population (282 individuals), a tight cluster of nine markers (barc124, wmc407, gwm636, cfd36, wmc382, gwm512, wmc25, barc1138 and gwm400) in a 6 cM region represented the *Lr37/Yr17/Sr38* translocated segment in Jagger (Fang et al. 2011).

As some of the markers amplified null alleles in this study, unsuccessful amplification for a specific sample could have mistakenly been recorded as a null allele, resulting in the detection of a potential false recombination event causing a longer than expected linkage map. Rare events of possible recombination between molecular markers and *Lr37/Yr17/*Sr38 were reported by Robert et al. (2000), although Fang et al. (2011) and Gao et al. (2021) reported the translocation to be non-recombining with wheat. Helguera et al. (2003) could not rule out a potential recombination event outside the region covered with the RFLP markers as a probable cause for the lack of resistance in backcross material they developed in Anza, which retained the translocated segment marker alleles but were susceptible. They however found the evidence of a possible suppressor gene in Anza to be a more plausible explanation for the lack of resistance in these lines. Analysis of the 35K Affymetrix Axiom™ Wheat Breeders' Array data indicated that 2014 and 2019 seed sources of RIL#157 and #163 for which recombination events were recorded in the *QYr.ufs-2A.2(Yr17)* interval (Table 1) showed a disproportionally large number of unaccounted parental allele calls (NoCall and AB) on the group 2 chromosomes in RIL#157 and on chromosome 2A in #163. Regardless of this, the phenotypes of these lines were in line with the rest of the RIL population and were reported to be carriers of the *QYr.ufs-2A.2 (Yr17)* QTL based on the SSR marker alleles spanning the interval. Further investigation is required to determine the origin of these non-parental SNP alleles.

In contrast to the SSR markers and dominant SNP markers derived from the 90K Illumina wheat SNP chip used by Xue et al. (2018), where the absence of an allele was associated with the *A. ventricosa* genome, the informative SNP markers identified in this study detected alleles of both the common wheat and *A. ventricosa* genomes. This is probably the result of the inclusion of translocations of wild wheat species in the development of the 35K Axiom Array (Winfield et al. 2016). Gao et al. (2021) performed an extensive cytological and physical characterisation of the $2N^VS$ translocation. They delineated the $2N^VS$ translocated segment to ~ 33 Mb region in the *Yr17*-carrying wheat cultivars Jagger and CDC Stanley, which is slightly larger than the estimated size of 27.8 Mb based on genetic mapping and positioning on the wild emmer wheat reference genome (Avni et al. 2017; Xue et al. 2018). In this study, it was confirmed that the most terminal part of the NSRPan4 wheat genome 2AS (~ 20 Mb in the CS genome) was replaced by a ~ 29 Mb *A. ventricosa* segment with the breakpoint somewhere in the region proximal to wmc25c. It is in concordance with the findings of Gao et al. (2021) who stated that the translocation increased the size of 2A with ~ 9 Mb. This large gene-rich region in Jagger was shown to carry more than 10% NLR-type genes as expected for a telomeric region carrying resistance to many different pathogens and potentially also more than one gene to a specific pathogen.

In this study, depending on the score and season, the *QYr.ufs-2A.2(Yr17)* interval explained up to 23.5% of the total phenotypic variance observed in the SIT score generated with a virulent *Yr17* pathotype. Despite the observed virulence for *Lr37/Yr17/Sr38*, several studies reported environmental interactions in seedling tests and field resistance in lines carrying the gene in combination with others (Bariana and McIntosh 1994; Hovmøller 2007; Milus et al. 2015). These include reports of wheat cultivars, containing *Yr17*, that are intermediate to susceptible in the seedling stage with APR to the same isolates (Dedryver et al. 2009; Fang et al. 2011; Milus et al. 2015). Similarly in this study Trident (*Lr37/Yr17/Sr38; Sr12, Sr5, Sr8a/b*; Park et al. 2009) gave a 30R field reading for the seedling virulent pathotype 6E22A + and the phenotype of Yr17/6*Avocet S in the field was also not indicative of full susceptibility. Fang et al. (2011) questioned the strict conventional perception of the understanding of resistance gene sources and commented that race-specific APR genes should also be considered as the evidence in their study suggested for *Yr17*. The *QYr.ufs-2A.2(Yr17)* interval covers the fairly large distal region from gwm210a to gwm512 (24.3 cM), and it is not possible to infer whether another gene associated with the $2N^VS$ segment may lie within the QTL interval detected. Analysis of the SNP calls confirmed the SSR haplotypes of RIL#167 being a *QYr.ufs-2A.2(Yr17)* carrier and RIL#14, RIL#59, RIL#158 and RIL#165 as non-carriers. The latter four RILS expressed mostly intermediate SITs, and moderate (MS) to resistant (MRR) field ratings.

Similar to the *QYr.ufs-2A.2(Yr17)* region, the analysis clearly detected a seedling response in the *QYr.ufs-2B.1* interval flanked by BS00110209 and wmc317 in the distal part of 2BL. Known seedling resistance genes on 2B that are ruled out as they are located on the short arm include: *Yr27* (Selkirk); *Yr31*; *YrV23*; *YrSp*; *YrTpl* and *YrCN19* (Luo et al. 2009). *Yr5, Yr7* and *YrQz* (Luo et al. 2009) are seedling resistance genes on the long arm of this chromosome. The line *Yr5*/6*Avocet S typically has a 0; SIT against SA *Pst* pathotype 6E22A + compared to the ;1c score of NSRPan4. In contrast to what is expected from a major seedling resistance gene, the phenotypic variance explained by *QYr.ufs-2B.1* for the SIT _1–9 was 46.4%. There are no APR genes on 2BL according to the wheat gene catalogue (McIntosh et al. 2017), but there are some QTL indicated on MASwheat. Basnet et al. (2014) identified *QYr.tam-2BL* in TAM 111 which explained between 13 and 63% of the total phenotypic variance observed for DS. Similar to *QYr.ufs-2B.1*, it mapped to the distal part of 2BL south of gwm501 and also detected a seedling response. It explained 40.5% of the total phenotypic variance observed for the seedling score, which is comparable with the 46.4% observed for *QYr.ufs-2B.1.*

The *QYr.ufs-2B.1* interval covers over a fairly large area of approximately 45 cM (112.3 Mb) (IWGS2018). This area may either contain more than one resistance gene, or *QYr.ufs-2B.1* confers a form of partial resistance at seedling and adult plant level. FR for RILs carrying only the *QYr.ufs-2B.1* interval and which exhibited low to intermediate SITs (1c to 2c), varied mostly between 20MRMS and 40MRMS over seasons. It appears that the SIT effect observed for *QYr.ufs-2B.1* resulted in moderate levels of APR. Herrera-Foessel et al. (2015) reported a similar effect for *Yr60* in Almop, a cultivar that exhibits moderate resistance to stripe rust in seedlings and adult plants.

The combined effect of the 2A and 2B regions in combination with unidentified or minor resistances in NSRPan4 are thus responsible for a much more resistant phenotype compared to Almop in which only *Yr60* was detected. Similar to this study, RILs were identified where the seedling and adult plant responses did not correlate and they concluded that the environmental effect is expected to be large for a gene that shows intermediate effect.

However, the fact that additional ASR and APR genes might be located on this large 2B chromosome segment cannot be ruled out. This is not unexpected considering the various reports on additional APR resistances detected in Milan (Feng et al. 2014, 2015), one of the parental lines of NSRPan4. SNP analysis supported the SSR haplotypes of RILs#14, #59, #158 and #165 as carriers of *QYr.ufs-2B.1* with the $2N^VS$ segment absent (Table 1).

Although a small effect in the range of 4.8–13.2% R^2 was observed on chromosome 1B (*QYr.ufs-1B.1)*, for the end of season LAI and RT scores in 2015 and 2016 and the GS score of 2016 (Table 2), it is noteworthy that this QTL maps in the same region as the APR *Lr46/Yr29* gene and its presence cannot be ruled out. Lillemo et al. (2008) showed that *Lr46/Yr29* as represented by the wmc719 - Xhbe248 interval explained 17.4% of the stripe rust phenotypic variation

observed in the severity score of the CIMMYT wheat Saar, while it was not clearly detected by Navabi et al. (2003). This interval falls within the cfa2292.1 and barc80 *QYr.ufs-1B.1* interval. Wmc44 and barc80 are amongst the markers recommended by MASwheat (http://maswheat.ucdavis.edu/protocols/Lr46) to track *Lr46/Yr29*. Unfortunately, the respective marker alleles associated with this gene have proven to be prevalent in many wheat populations from different regions and can only be regarded as diagnostic when used in an informative cross with a known *Lr46/Yr29* carrier such as Pavon 76 (Prins et al. 2016; ES Lagudah personal communication). Lillemo et al. (2008) reported that *Lr46/Yr29* explained 17% of the phenotypic variation in the severity score, whilst the highest R^2 for severity in this study for *QYr.ufs-1B.1* was only 6.9% (LAI_29SEPT16). A higher R^2 of 13.2% was observed for the RT_01OCT15 score. This QTL was not detected with the SIT score supporting an APR status. Lillemo et al. (2008) also noted that when *Lr46/Yr29* was in the presence of *Lr34/Yr18*, its additive effect on leaf rust resistance was much less showing the effect of genetic interactions on some of the resistance genes.

The detection of the *QYr.ufs-2A.2(Yr17)* in this line is an important finding, since the $2N^{V}S$ segment is known to be an agronomically important translocation. In addition to the yield benefit associated with it (Gao et al. 2021), the multiple disease and nematode resistance genes it carries (Jahier et al. 2001; Williamson et al. 2013), it also confers resistance to the *Triticum* pathotype of *Magnaporthe oryzae* causing wheat blast (Cruz et al. 2016). Wheat blast is a new threat to wheat production in Africa (Tembo et al. 2020) and as this segment is already utilised by South African wheat breeders it can serve as the basis to add other wheat blast resistance genes to (Cruz et al. 2016) in a pre-emptive step to manage this devastating threat.

Conclusion

QTL analysis identified stripe rust resistance genes/QTL with a consistent seedling and adult plant effect on chromosomes 2A and 2B. Despite the reported virulence for *Yr17*, *QYr.ufs-2A.2(Yr17)* contributed towards the observed FR and SIT resistance observed in the population. This study confirmed the various reports that *Yr17*-carrying segment either carries more resistance components to stripe rust or is influenced by environmental factors, pathotype and genetic background. *QYr.ufs-2B.1* contributed towards a lower FR, but a larger SIT effect. As revealed by the total R^2 explained and the difference in responses of specific resistant and susceptible subsets containing none of the major QTL, it is clear that there are still unidentified resistance components at play. Although inconsistently detected, *QYr.ufs-1B.1* could possibly be the *Lr46/Yr29* gene and a contributor towards resistance in the RILs not carrying *QYr.ufs-2A.2(Yr17)* or *QYr.ufs-2B.1*. Combined, the identified QTL and unknown resistance provide the comprehensive field resistance that is consistently observed for NSRPan4. Marker coverage of chromosomes 4A, 6A and 6B will be increased to improve chances to detect possible additional Milan-derived genes.

References

Allen AM, Winfield MO, Burridge AJ, Downie RC, Benbow HR, Barker GLA, Wilkinson PA, Coghill J, Waterfall C, Davassi A, Scopes G, Pirani A, Webster T, Brew F, Bloor C, Griffiths S, Bentley AR, Alda M, Jack P, Phillips AL, Edwards KJ (2017) Characterization of a Wheat Breeders' Array suitable for high-throughput SNP genotyping of global accessions for hexaploid bread wheat (*Triticum aestivum*). Plant Biotech J 15:390–401. https://doi.org/10.1111/pbi.12635

Agenbag GM, Pretorius ZA, Boyd LA, Bender CM, MacCormack R, Prins R (2014) High-resolution mapping and new marker development for adult plant stripe rust resistance QTL in the wheat cultivar Kariega. Mol Breed 34(4):2005–2020. https://doi.org/10.1007/s11032-014-0158-4

Agenbag GM, Pretorius ZA, Boyd LA, Bender CM, Prins R (2012) Identification of adult plant resistance to stripe rust in the wheat cultivar Cappelle-Desprez. Theor Appl Genet 125:109–120. https://doi.org/10.1007/s00122-012-1819-5

Appels T (2003) A consensus molecular genetic map for wheat - a cooperative international effort. In: Pogna NE, McIntosh RA (eds) Proceedings of the 10th International Wheat Genetics Symposium, 1-6 September, Paestum, Italy. Istituto Sperimentale per la Cerealicoltura, Rome, pp 211–214

Athiyannan N, Abrouk M, Boshoff WHP, Cauet S, Rodde N, Kudrna D, Mohammed N, Bettgenhaeuser J, Botha K, Derman S, Wing RA, Prins R, Krattinger SG (2022) Long-read bread wheat genome enables disease resistance gene cloning. Nat Genet 54:227–231. https://doi.org/10.1038/s41588-022-01022-1

Avni R, Nave M, Barad O, Baruch K, Twardziok et al (2017) Wild emmer genome architecture and diversity elucidate wheat evolution and domestication. Science 357:93–97. https://doi.org/10.1126/science.aan0032

Bariana HS, McIntosh RA (1993) Cytogenetic studies in wheat. XV. Location of rust resistance genes in VPM1 and their genetic linkage with other disease resistance genes in chromosome 2A. Genome 36:476–482. https://doi.org/10.1139/g93-065

Bariana HS, McIntosh RA (1994) Characterisation and origin of rust and powdery mildew resistance genes in VPM1 wheat. Euphytica 76:53–61. https://doi.org/10.1007/BF00024020

Basnet BR, Ibrahim AMH, Chen X, Singh RP, Mason ER, Bowden RL, Liu S, Hays DB, Devkota RN, Subramanian NK, Rudd JC (2014) Molecular Mapping of Stripe Rust Resistance in Hard Red Winter Wheat TAM 111 Adapted to the U.S. High Plains. Crop Sci 54:1361–1373. https://doi.org/10.2135/cropsci2013.09.0625

Bayles RA, Flath K, Hovmøller MS, De Vallavieille-Pope C (2000) Breakdown of the *Yr17* resistance to yellow rust of wheat in northern Europe. Agronomie 20:805–811. https://doi.org/10.1051/agro:2000176

Bhavani S, Hodson DP, Huerta-Espino J, Randhawa MS, Singh RP (2019) Progress in breeding for resistance to Ug99 and other races of the stem rust fungus in CIMMYT wheat germplasm. Front. Agr Sci Eng 6(3):210–224. https://doi.org/10.15302/J-FASE-2019268

Chen X (2013) High-temperature adult-plant resistance, key for sustainable control of stripe rust. Am J Plant Sci 04:608–627. https://doi.org/10.4236/ajps.2013.43080

Chen X (2020) Pathogens which threaten food security: *Puccinia striiformis*, the wheat stripe rust pathogen. Food Sec 12:239–251. https://doi.org/10.1007/s12571-020-01016-z

Cruz CD, Peterson GL, Bockus WW, Kankala P, Dubcovsky J, Jordan KW, Akhunov E, Chumley F, Baldemolar FD, Valent B (2016) The 2NS translocation from *Aegilops ventricosa* confers resistance to the *Triticum* pathotype of *Magnaporthe oryzae*. Crop Sci 56:990–1000. https://doi.org/10.2135/cropsci2015.07.0410

Dedryver F, Paillard S, Mallard S, Robert O, Trottet M, Nègre S, Verplancke G, Jahier J (2009) Characterization of genetic components involved in durable resistance to stripe rust in the bread wheat 'Renan'. Phytopathology 99(8):968–973. https://doi.org/10.1094/PHYTO-99-8-0968

Doyle JJ, Doyle JL (1990) A rapid total DNA preparation procedure for fresh plant tissue. Focus 12:13–15

Dubcovsky J, Luo M-C, Zhong G-Y, Bransteiter R, Desai A, Kilian A, Kleinhofs A, Dvorak J (1996) Genetic map of diploid wheat, *Triticum monococcum* L., and its comparison with maps of *Hordeum vulgare* L. Genetics 143:983–999. https://doi.org/10.1093/genetics/143.2.983

Fang T, Campbell KG, Liu Z et al (2011) Stripe rust resistance in the wheat cultivar Jagger is due to *Yr17* and a novel resistance gene. Crop Sci 51:2455–2465. https://doi.org/10.2135/cropsci2011.03.0161

Feng J, Chen G, Wei Y, Liu Y, Jiang Q, Li W, Pu Z, Lan X, Dai S, Zheng Y (2014) Identification and genetic mapping of a recessive gene for resistance to stripe rust in wheat line LM168-1. Mol Breed 33:601–609. https://doi.org/10.1007/s11032-013-9977-y

Feng JY, Wang MN, Chen XM, See DR, Zheng YL, Chao SM, Wan AM (2015) Molecular mapping of *YrSP* and its relationship with other genes for stripe rust resistance in wheat chromosome 2BL. Phytopathology 105(9):1206–13. https://doi.org/10.1094/PHYTO-03-15-0060-R

Gao L, Koo D-H, Juliana P, Rife T, Singh D, Lemes da Silva C, Lux T, Dorn KM, Clinesmith M, Silva P, Wang X, Spannagl M, Monat C, Friebe B, Steuernagel B, Muehlbauer, Walkowiak S Pzaniak C, Singh R, Stein N, Mascher M, Fritz A, Poland J (2021). The *Aegilops ventricosa* $2N^{V}S$ segment in bread wheat: cytology, genomics and breeding. Theor and Appl Genet 134:529–542. https://doi.org/10.1007/s00122-020-03712-y

Guzmán C, Autrique E, Mondal S, Huerta-Espino J, Singh RP, Vargas M, Crossa J, Amaya A, Peña RJ (2017) Genetic improvement of grain quality traits for CIMMYT semi-dwarf spring bread wheat varieties developed during 1965–2015: 50 years of breeding. Field Crops Res 210:192–196. https://doi.org/10.1016/j.fcr.2017.06.002

Helguera M, Khan IA, Kolmer J, Lijavetzky D, Zhong-qi L, Dubcovsky J (2003) PCR assays for the *Lr37-Yr17-Sr38* cluster of rust resistance genes and their use to develop isogenic hard red spring wheat lines. Crop Sci 43:1839–1847. https://doi.org/10.2135/cropsci2003.1839

Herrera-Foessel SA, Singh RP, Lan CX, Huerta-Espino J, Calvo-Salazar V, Bansal UK, Bariana HS, Lagudah ES (2015) *Yr60*, a gene conferring moderate resistance to stripe rust in wheat. Plant Dis 99(4):508–511. https://doi.org/10.1094/PDIS-08-14-0796-RE

Hovmøller MS (2007) Sources of seedling and adult plant resistance to *Puccinia striiformis* f. sp. *tritici* in European wheats. Plant Breed 126(3):225–233. https://doi.org/10.1111/j.1439-0523.2007.01369.x

Huerta-Espino J, Singh R, Crespo-Herrera LA., Villaseñor-Mir HE, Rodriguez-Garcia MF, Dreisigacker S, Barcenas-Santana D, Lagudah E (2020) Adult plant slow rusting genes confer high levels of resistance to rusts in bread wheat cultivars from Mexico. Front Plant Sc 11:824. https://doi.org/10.3389/fpls.2020.00824

IWGSC (2018) Shifting the limits in wheat research and breeding using a fully annotated reference genome. Science 361:661. https://doi.org/10.1126/science.aar7191

Jaganathan D, Bohra A, Thudi M, Varshney RK (2020) Fine mapping and gene cloning in the post-NGS era: advances and prospects. Theor and Appl Genet 133:1791–1810. https://doi.org/10.1007/s00122-020-03560-w

Jahier A, Tanguy D, Rivoal K, Bariana HS (2001) The *Aegilops ventricosa* segment on chromosome 2AS of the wheat cultivar 'VPM1' carries the cereal cyst nematode resistance gene *Cre5*. Plant Breed 120:125–128. https://doi.org/10.1046/j.1439-0523.2001.00585.x

Juliana P, Singh RP, Huerta-Espino J, Bhavani S, Randhawa MS, Kumar U, Joshi AK, Bhati PK, Villaseñor-Mir HE, Mishra CN, Singh GP (2020) Genome-wide mapping and allelic fingerprinting provide insights into the genetics of resistance to wheat stripe rust in India, Kenya and Mexico. Sci Rep 10:10908. https://doi.org/10.1038/s41598-020-67874-x

Li J, Dundas I, Dong C, Li G, Trethowan R, Yang Z, Hoxha S, Zhang P (2020) Identification and characterization of a new stripe rust resistance gene *Yr83* on rye chromosome 6R in wheat. Theor Appl Genet 133:1095–1107. https://doi.org/10.1007/s00122-020-03534-y

Lillemo M, Asalf B, Singh RP, Huerta-Espino J, Chen XM, He ZH, Bjørnstad Å (2008) The adult plant rust resistance loci *Lr34/Yr18* and *Lr46/Yr29* are important determinants of partial resistance to powdery mildew in bread wheat line Saar. Theor Appl Genet 116(8):1155–66. https://doi.org/10.1007/s00122-008-0743-1

Line RF, Chen X (1995) Successes in breeding for and managing durable resistance to wheat rusts. Plant Dis 79:1254–1255

Luo P, Hu X, Zhang H, Ren Z (2009) Genes for resistance to stripe rust on chromosome 2B and their application in wheat breeding. Progr Nat Sci 19:9–15. https://doi.org/10.1016/j.pnsc.2008.02.017

Maia N (1967) Obtention de blés tendres résistants au piétin-verse par croisement interspécifiques blés X Aegilops. C R Acad Agric Fr 53:149–154

McIntosh RA, Dubcovsky J, Rogers WJ, Morris C, Xia XC (2017) Catalogue of gene symbols for wheat: 2017 supplement. https://wheat.pw.usda.gov/GG3/maps. Accessed 12 July 2022

McIntosh RA, Wellings CR, Park RF (1995) Wheat rusts - an atlas of resistance genes. CSIRO, Melbourne (Australia): CSIRO Publishing.

Milus EA, Lee KD, Brown-Guedira G (2015) Characterization of stripe rust resistance in wheat lines with resistance gene Y*r17* and implications for evaluating resistance and virulence. Phytopathology 105(8):1123–30. https://doi.org/10.1094/PHYTO-11-14-0304-R

Navabi A, Singh RP, Tewari JP, Briggs KG (2003) Genetic analysis of adult-plant resistance to leaf rust in five spring wheat genotypes. Plant Dis 87(12):1522–1529. https://doi.org/10.1094/PDIS.2003.87.12.1522

Qayoum A and Line RF (1985) High-temperature adult-plant resistance to stripe rust of wheat. Phytopathology 75:1121–1125. https://doi.org/10.1094/Phyto-75-1121

Park R, Wellings C, Bariana H, Bansal U (2009) Australia cereal cultivar pedigree and seedling rust genotype information. The University of Sydney, Plant Breeding Institute. Cereal Rust Report Season 7(2):9

Peterson, RF, Champbell, AB, Hannah, AE (1948) A diagrammatic scale for estimating rust intensity of leaves and stem of cereals. Can J Res 26:496–500. https://doi.org/10.1139/cjr48c-033

Pretorius ZA, Lan CX, Prins R, Knight V, McLaren NW, Singh RP, Bender CM, Kloppers FJ (2017) Application of remote sensing to identify adult plant resistance loci to stripe rust in two bread wheat mapping populations. Precis Agr 18(4):411–428. https://doi.org/10.1007/s11119-016-9461-x

Pretorius ZA, Pakendorf KW, Marais GF, Prins R, Komen JS (2007) Challenges for sustainable cereal rust control in South Africa. Aust J Agr Res 58:593–601. https://doi.org/10.1071/AR06144

Prins R, Dreisigacker S, Pretorius ZA, Van Schalkwyk H, Wessels E, Smit C, Bender C, Singh D, Boyd LA (2016) Stem rust resistance in a geographically diverse collection of spring wheat lines collected from across Africa. Front Plant Sci 7:973. https://doi.org/10.3389/fpls.2016.00973

Prins R, Pretorius ZA, Bender CM, Lehmensiek A (2011) QTL mapping of stripe, leaf and stem rust resistance genes in a Kariega x Avocet S doubled haploid wheat population. Mol Breed 27:259–270. https://doi.org/10.1007/s11032-010-9428-y

R Core Team (2013) R: A language and environment for statistical computing. R Foundation for Statistical Computing, Vienna, Austria. http://www.R-project.org/. Accessed 12 July 2022

Ramburan VP, Pretorius ZA, Louw JH, Boyd LA, Smith PH, Boshoff WHP, Prins R (2004) A genetic analysis of adult plant resistance to stripe rust in the wheat cultivar Kariega. Theor Appl Genet 108:1426–1433. https://doi.org/10.1007/s00122-003-1567-7

Robert O, Dedryver F, Leconte M, Rolland B, De Vallavieille-Pope C (2000) Combination of resistance tests and molecular tests to postulate the yellow rust resistance gene *Yr17* in bread wheat lines. Plant Breed 119:467–472. https://doi.org/10.1046/j.1439-0523.2000.00530.x

Rosewarne GM, Herrera-Foessel SA, Singh RP, Huerta-Espino J, Lan CX, He ZH (2013) Quantitative trait loci of stripe rust resistance in wheat. Theor Appl Genet 126:2427–49. https://doi.org/10.1007/s00122-013-2159-9

Rosewarne GM, Singh RP, Huerta-Espino J, William HM, Bouchet S, Cloutier S, McFadden H, Lagudah ES (2006) Leaf tip necrosis, molecular markers and *β*1-proteasome subunits associated with the slow rusting resistance genes *Lr46/Yr29*. Theor Appl Genet 112:500–508. https://doi.org/10.1007/s00122-005-0153-6

Shah IA (2015) Evaluation of elite bread wheat genotypes for grain yield and other agronomic attributes. Acad J Biotechnol 3(1):6–9

Sharma-Poudyal D, Chen XM, Wan AM, Zhan GM, Kang ZS, Cao SQ, Jin SL, Morgounov A, Akin B, Mert Z, Shah SJA, Bux H, Ashraf M, Sharma RC, Madariaga R, Puri KD, Wellings C, Xi KQ, Wanyera R, Manninger K, Ganzáles MI, Koyda M, Sanin S, Patzek LJ (2013) Virulence characterization of international collections of the wheat stripe rust pathogen, *Puccinia striiformis* f. sp. *tritici*. Plant Dis 97:379–386. https://doi.org/10.1094/PDIS-01-12-0078-RE

Smith PH, Hadfield J, Hart NJ, Koebner RMD, Boyd LA (2007) STS markers for the wheat yellow rust resistance gene *Yr5* suggest a NBS-LRR-type resistance gene cluster. Genome 50(3):259–265. https://doi.org/10.1139/G07-004

Suenaga K, Singh RP, Huerta-Espino J, William HM (2003) Microsatellite markers for genes *Lr34/Yr18* and other quantitative trait loci for leaf rust and stripe rust resistance in bread wheat. Phytopathology 93(7):881–890. https://doi.org/10.1094/PHYTO.2003.93.7.881

Sun Q, Wei Y, Ni Z, Xie C, Yang T (2002) Microsatellite marker for yellow rust resistance gene *Yr5* in wheat introgressed from spelt wheat. Plant Breed 121(6):539–541. https://doi.org/10.1046/j.1439-0523.2002.00754.x

Tembo B, Mulenga RM, Sichilima S, M'siska KK, Mwale M, Chikoti PC, Singh PK, He X, Kerry F, Pedley KF, Peterson GL, Singh RP, Braun HJ (2020) Detection and characterization of fungus (*Magnaporthe oryzae* pathotype *Triticum*) causing wheat blast disease on rain-fed grown wheat (*Triticum aestivum* L.) in Zambia. PLoS ONE 15(9):e0238724. https://doi.org/10.1371/journal.pone.0238724

Visser B, Herselman L, Pretorius ZA (2016) Microsatellite characterisation of South African *Puccinia striiformis* races. SA J of Plant and Soil 33(3):161–166. https://doi.org/10.1080/02571862.2015.1125957

Voorrips RE (2002) MapChart: Software for the graphical presentation of linkage maps and QTLs. J Hered 93(1):77–78. https://doi.org/10.1093/jhered/93.1.77

Walkowiak S, Gao L, Monat C et al (2020) Multiple wheat genomes reveal global variation on modern breeding. Nature 588:277–283. https://doi.org/10.1038/s41586-020-2961-x

Walter S, Ali S, Kemen E, Nazari K, Bahri B, Enjalbert Hansen JG, Brown JK, Sicheritz-Pontén T, Jones J, de Vallvieille-Pope C, Hovmøller MS, Justesen AF (2016) Molecular markers for tracking the origin and worldwide distribution of invasive strains of *Puccinia striiformis*. Ecol Evol 6:2790–2804. https://doi.org/10.1002/ece3.2069

Wang S, Basten CJ, Zeng ZB (2012) Windows QTL Cartographer 2.5. Department of Statistics, North Carolina State University, Raleigh, North Carolina, http://statgen.ncsu.edu/qtlcart/WQTLCart.htm. Accessed 12 July 2022

Wang MN, Chen XM (2017) Stripe rust resistance. In Stripe Rust, 5th ed.; Chen, X.M., Kang, Z.S., Eds.; Springer: Dordrecht, The Netherlands, pp. 353–558

Wessels E, Prins R (2017) Development of a low resolution genome scan marker set for the acceleration of major gene or QTL mapping in wheat. SA J of Plant and Soil 34(2):155–158. https://doi.org/10.1080/02571862.2016.1201156

Wessels E, Prins R Boshoff WHP, Zurn JD, Acevedo M, Pretorius ZA (2019) Mapping a resistance gene to *Puccinia graminis* f. sp. *tritici* in the bread wheat cultivar Matlabas. Plant Dis 109(9):2337–2344. https://doi.org/10.1094/PDIS-10-18-1731-RE

Wilkinson PA, Winfield MO, Barker GLA, Allen AM, Burridge A, Coghill JA, Edwards KJ (2012) CerealsDB 2.0: an integrated resource for plant breeders and scientists. BMC Bioinformatics 13:219. https://doi.org/10.1186/1471-2105-13-219

Williamson VM, Thomas V, Ferris H, Dubcovsky J (2013) An *Aegilops ventricosa* translocation confers resistance against root-knot nematodes to common wheat. Crop Sci 53:1412–1418. https://doi.org/10.2135/cropsci2012.12.0681

Wickham H (2016) ggplot2: Elegant Graphics for Data Analysis. Springer-Verlag New York, New York.

Winfield M.O, Allen AM, Burridge AJ, Barker GLA, Benbow HR, Wilkinson PA, Coghill J, Waterfall C, Davassi A, Scopes G, Pirani A, Webster T, Brew F, Bloor C, King J, West C, Griffiths S, King I, Bentley AR, Edwards KJ (2016) High-density SNP genotyping array for hexaploid wheat and its secondary and tertiary gene pool. Plant Biotechnol J 14:1195–1206. https://doi.org/10.1111/pbi.12485

Xue S, Kolmer JA, Wang S, Yan L (2018) Mapping of leaf rust resistance genes and molecular characterization of the 2NS/2AS translocation in the wheat cultivar Jagger. G3 8:2059–2065. https://doi.org/10.1534/g3.118.200058

Declarations

Funding The South African Winter Cereal Trust is thanked for funding (WCT/W/2015/02). The National Research Foundation is thanked for Incentive Funding (UID#85943). PANNAR SEED (Pty) Ltd is thanked for the maintenance of field trials.

Competing interests The authors declare that they have no financial or non-financial conflict of interest.

Author contributions WHPB selected the CIMMYT line for genetic analysis. ZAP and CMB developed the RIL population, ZAP, CMB and WHPB performed field and greenhouse phenotyping and analysis of disease data. CdK conducted all molecular experiments, QTL analysis and wrote the first draft, KB and EW conducted the SNP array analyses. ZAP, EW and WHPB co-wrote the article along with RP who coordinated the project and provided major inputs in preparation of the final manuscript.

Data availability Most of the datasets generated during and/or analysed during the current study are available in the online resources. The 35K Affymetrix Axiom^{TM} Wheat Breeders' Array data can be requested from the corresponding author.

Tables

Table 1 Marker haplotypes representing *QYr.ufs-2A.2*(*Yr17*) and *QYr.ufs-2B.1* for RILs and control lines selected for the 35K Axiom^{TM} Array analysis

Entry[a]	*QYr.ufs-2A.2*(*Yr17*)															
	[c]gwm210a	**Lr37/Yr17/Sr38**	**gpw4108**	**xib58**	wmc25c	BS00021691	gpw7101	wmc407	xib125c	xib27b	gwm210b	barc212	[c]gwm512	gwm501	BS00009989	cf
NSRPan4	A	A	A	A	A	A	A	A	A	A	A	A	A	A	A	
Avocet S	B	B	B	B	B	B	B	B	B	B	B	B	B	B	B	
RIL#167	A	A	A	A	A	A	A	A	A	A	A	A	B	A	A	
RIL#157[b]	A	B	B	B	B	B	A	A	A	A	A	A	A	B	B	
RIL#163[b]	A	B	B	B	B	B	A	A	A	A	A	A	A	B	B	
RIL#014	B	B	B	B	B	B	B	B	B	B	B	B	B	A	A	
RIL#059	A	B	B	B	B	B	B	B	B	B	B	B	B	A	A	
RIL#158	B	B	B	B	B	B	B	B	B	B	B	B	B	A	A	
RIL#165	A	B	B	B	B	B	B	B	B	B	B	B	B	A	A	

[a]All RIL entries represent mapping population RIL F_6 NSRPan4 x Avocet S individuals

[b]Seed sources of 2014 and 2019 were included for these RILs

[c]Markers flanking *QYr.ufs-2A.2(Yr17)* interval; markers in bold represent *Lr37/Yr17/Sr38* translocated segment within that interval

[d]Two markers most significantly associated with *QYr.ufs-2B.1* and used to determine its presence/absence

Table 2 Stripe rust resistance QTL detected in the RIL population of NSRPan4 x Avocet S for leaf area infected (LAI), host reaction type (RT), leaf damage (GS) and seedling infection type (SIT) scores using *Puccinia striiformis* f. sp *tritici* pathotype 6E22A+. The origin of all detected QTL was NSRPan4

					2014				2015		
QTL name	Significant QTL interval	Most significantly associated markers	Chr[a]		LAI_02OCT14	RT_02OCT14	LAI_16OCT14	RT_16OCT14	LAI_17SEPT15avg	RT_17SEPT15avg	LAI_01OCT15a
QYr.ufs-1B.1	cfa2219a - barc80	cfa2219a - wmc44*	1B	LOD							4.2
				% Var							6.0
QYr.ufs-2A.2(*Yr17*)	gwm210a - gwm512	gwm210a - gwm210b*	2A	LOD	10.0	16.8	15.0	11.8	19.4	18.7	25.1
				% Var	24.3	40.0	31.6	32.4	41.9	48.6	54.5
QYr.ufs-2B.1	gwm501 - wmc317	BS00110209 - BS00022064*	2B	LOD	3.4	5.5	7.4	8.9	5.8	5.2	5.4
				% Var	6.5	22.3	16.3	27.1	13.8	13.9	11.2
QYr.ufs-3D.1	barc125 - cfd34	cfd4	3D	LOD							
				% Var							
QYr.ufs-7A.1	gwm276 - wmc422	wmc422	7A	LOD			3.1				
				% Var			5.0				
Total R^2				∑	30.8	62.3	52.9	59.5	55.7	62.5	71.6

*The most significantly associated marker for the different traits varied in the indicated interval

[a]Chromosome

Figures

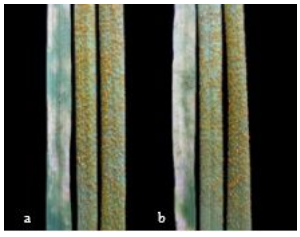

Figure 1

Lr37/Yr17/Sr38 seedling phenotypic tests. **a** From left to right: NSRPan4, Avocet S, Trident infected with 6E16A- **b** From left to right: NSRPan4, Avocet S, Trident infected with 6E22A+

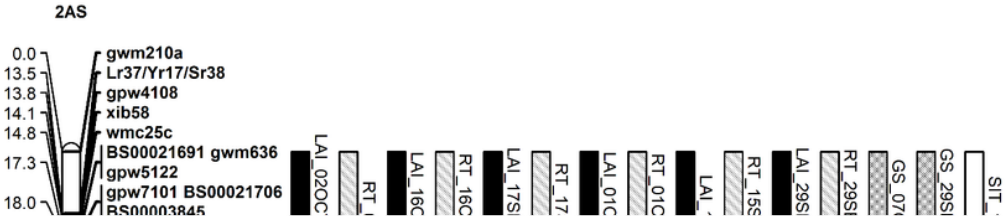

Figure 2

Stripe rust resistance *QYr.ufs-2A.2(Yr17)* detected on chromosome 2AS in the wheat cross NSRPan4 x Avocet S (markers in bold = significant LOD interval)

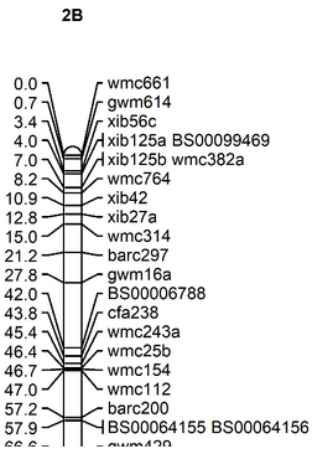

Figure 3

Stripe rust resistance *QYr.ufs-2B.1* detected on chromosome 2B in the wheat cross NSRPan4 x Avocet S (markers in bold = significant LOD interval)

Supplementary Files

This is a list of supplementary files associated with this preprint. Click to download.

- ESMOnlineresource1.xlsx
- ESMOnlineresource2.docx
- ESMOnlineresource3.xlsx
- ESMOnlineresource4.docx
- ESMOnlineresource5.docx
- ESMOnlineresource6.docx
- ESMOnlineresource7.docx